ISIJ International, Vol. 61 (2021), No. 1, pp. 380–386
https://doi.org/10.2355/isijinternational.ISIJINT-2020-137

Quantification of the Severity of Ridging in Ferritic Stainless Steel Sheets Using a Profilometric Technique

Suresh KODUKULA,[1,3)]* Thomas OHLIGSCHLÄGER[2)] and David PORTER[3)]

1) Outokumpu Process R&D, Tornio, 95490 Finland.
2) VTT Technical Research Center of Finland Ltd, VTT, 02044 Finland.
3) Materials and Mechanical Engineering, Centre for Advanced Steels Research, University of Oulu, Oulu, 90014 Finland.

(*Received on March 18, 2020; accepted on July 15, 2020; J-STAGE Advance published date: September 11, 2020*)

A new method to quantify the ridging phenomenon in ferritic stainless steels has been developed based on the evaluation of surface profiles after the tensile elongation of 100 mm wide sheet specimens. The ridging components of the surface profiles are extracted by a tailored spline filtering procedure. A ridging index is proposed to quantify the severity of the surface defect based on surface profile height and spacing parameters. The procedure is independent of the type of profilometer used as long as unfiltered raw profiles can be recorded. The reproducibility of the measurement method and its correlation with the visual assessment of strained specimens is discussed.

KEY WORDS: ferritic stainless steels; ridging; ridging index; surface profile; spline filtering.

1. Introduction

Ferritic stainless steels (FSS) are widely used to produce goods that need high corrosion resistance and an excellent surface appearance. For the fabrication of dishes, pots and sinks from FSS sheet material, deep-drawing is usually the forming method of choice. Sometimes, also stretch-forming is applied. Despite having excellent forming properties, FSS are prone to the ridging surface defect which may appear on otherwise defect-free material after deep-drawing or stretching operations. Ridging is characterized by the formation of small parallel elevations and valleys which develop in the rolling direction when FSS sheet material is elongated. Ridging is at its highest when the material is strained along the rolling direction (RD) and absent when the sheet is elongated along the transverse direction (TD). The distance between two ridges is commonly in the range of a few millimeters. The additional profile height that is introduced by the ridging surface defect may be up to ± 50 μm depending on the applied strain.[1,2)] Consequently, additional mechanical polishing, which increases the production cost of the items, becomes necessary to achieve the often-needed high quality surface finish on the produced goods. The occurrence of the ridging surface defect is related to an unfavorable, inhomogeneous texture in the crystal structure of the strained FSS sheet.[3–8)] **Figure 1** presents photographs of a sample sheet strained parallel to TD and RD to illustrate the ridging surface defect.

In industrial practice, the occurrence of ridging is often assessed by a simple visual examination after sheet forming operations. When the deterioration of the surface quality is so strong that the required amount of polishing becomes unacceptable, the formed item may be rejected. For quality control purposes, a sample of the material may be strained to a defined elongation, typically between 7% and 20%. Then the samples, which are often about 20 mm wide standard tensile specimens, are rated visually based on a previously defined arbitrary scale, which typically varies from 1 to 5 or 1 to 10. This type of ridging assessment is usually done by specially trained personnel, often using a set of reference specimens. Therefore, the results are subjective and may be biased by the person doing the evaluation and the environment in which the rating takes place. For research purposes, the surface roughness profile of standard tensile test specimens after a defined elongation may be measured orthogonal to the straining direction. Ridging is then characterized by surface roughness parameters, which are typically determined according to common surface roughness measurement standards. Often the arithmetic average of the roughness profile Ra and/or the maximum height of the profile Rt are the measure for the intensity of ridging. Typically, the recorded raw profile is relatively short covering only a few ridges. This measured profile is then filtered according to surface roughness standards not considering

* Corresponding author: E-mail: suresh.kodukula@outokumpu.com

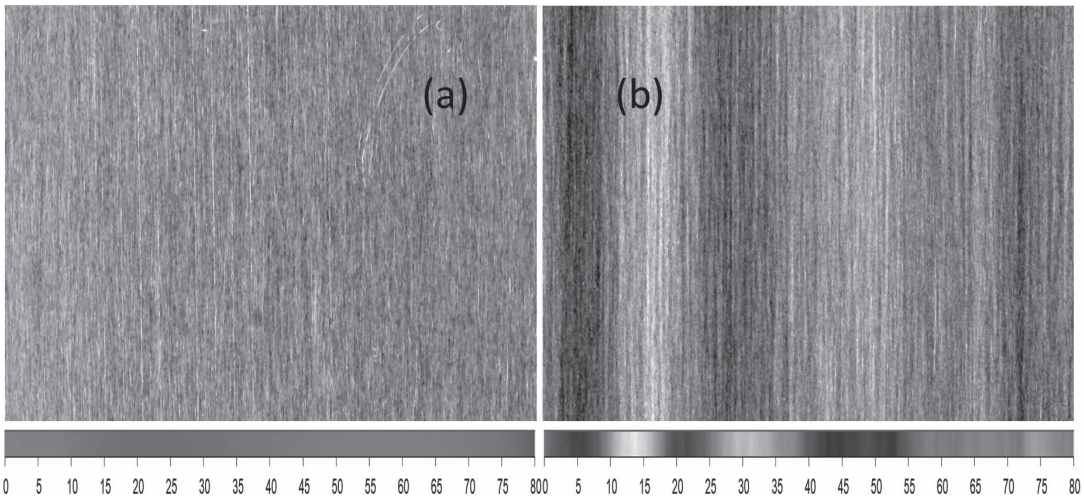

Fig. 1. Photographs and 3D surface profiles of 80 mm wide of grade EN 1.4016 FSS sample (a) before and (b) after 15% elongation parallel to RD showing the ridging surface defect. The scale of the 3D profiles varies between −50 μm (black) and +50 μm (white).

the special purpose of the measurement. Additionally, the spatial distribution of the ridges is rarely considered in these analyses.[7,9–11)]

A surface defect similar to ridging is roping, which is found in certain aluminum alloys used for instance in automotive applications. In contrast to FSS, the severity of roping is highest when the aluminum alloy is stretched parallel to TD. Surface profiling and similar surface roughness parameters as mentioned before for FSS have been proposed to quantify the extent of roping in aluminum alloys.[1,11–13)] However, Baczynsiki *et al.*[14)] could not find a correlation between the visual assessment of roping and these surface roughness parameters. To evaluate the as-rolled and deformation-induced surface roughness of Al sheets, Choi *et al.*[15)] introduced a modified roughness parameter (N%-*Rpv*) that depends upon the separate distribution of peaks and valleys. N%-*Rpv* is defined as the difference between the average heights of the upper N% of peaks and the lower N% of valleys. The authors suggested that the presence of deformation-induced macro-roughening patterns can be characterized using the relative magnitudes of 100%-*Rpv* and 10%-*Rpv* suggesting a possible link between the spatial distribution of surface roughness and the magnitude of N%-*Rpv*. However, Guillotin *et al.*[16)] reported that all of the above methods suffer from a lack of generalization because it seems that they all depend too much on data dimensions and step size. Instead, they proposed an areal power spectral density analysis method for the characterization of roping on aluminum alloys dividing the roping intensity into three levels: low, intermediate and high.

Ridging samples are often classified by visual inspection prior to manufacturing the products by deep drawing either to continue or reject the material which result in higher polishing costs. Published profilometric methods for the determination of the ridging intensity are mainly based on the determination of general surface roughness parameters like Ra or Rt after a defined elongation of the sheet sample in the RD. Due to the often-used short measurement lengths, the results may not be representative for the examined sheet material making it hard to evaluate ridging appropriately in terms of its amplitude and the spacing between the peaks and valleys. This qualitative measurement information of ridging also leads to difficulties in evaluating the influence of changes in process parameters. In this study, an improved profilometric characterization method is proposed. It combines a more suitable sample geometry with a tailored surface roughness filtering method that retains the relevant surface features. Then, a ridging index, which correlates well with visual inspection results, is calculated considering the profile height and the spatial distribution of the ridges.

2. Profilometric Ridging Measurement Method

2.1. Sample Preparation

Common profilometric methods for assessing the intensity of ridging on strained specimens are often based on standard surface roughness measurements of strained standard tensile specimens. The use of a standardized test methods simplifies the measurement procedure but limits the validity and reproducibility of the results at the same time. The width of standard tensile specimens after 15% straining is typically 17 mm, which is just enough to perform a standard surface roughness measurement. Considering that the profile height between ridges and valleys may be up to 50 μm, and that the filters used for separating the surface roughness profile from the raw profile demand an even longer traversing length, 12.5 mm is the maximum possible evaluation length for the surface roughness profile. As the distance between ridges is typically between 1 to 3 mm, usually only 4 to 12 complete surface features are included in such a measurement, which is not sufficient to characterize an FSS sheet with good statistical reliability. To overcome this limitation and to improve the confidence of the results, wider sheet specimens need to be used for profilometric ridging assessments.

In this study, industrially produced grades EN 1.4016 and EN 1.4509 FSS sheets with thicknesses between 0.5 and 1.5 mm served as test materials for the experiments. The surface condition was either cold rolled and skin-passed (2B) or bright annealed (2R). EN 1.4016 is an FSS with at least 16.0% Cr and normally a C content of 0.05% or less. This grade is commonly prone to the ridging surface defect. EN 1.4509 is a Ti and Nb dual stabilized FSS with lower

C content and at least 17.5% Cr. The intensity of ridging is often lower in stabilized FSS. Rectangular samples with a length of 300 mm and a width of 100 mm were strained at a rate of 1.5 mm/min until 1.5% elongation and then with 20 mm/min to 2%, 5%, 10% and 15% elongation using a ZwickRoell Z250 tensile testing machine equipped with custom-made clamps to hold the unusually wide samples. Most specimens were elongated parallel to RD to produce the ridging surface defect. Some samples were strained parallel to TD for comparison.

2.2. Surface Profile Acquisition

As ridging profiles not only consist of short wavelength roughness but also long wavelength components, it is important that the surface profiles are recorded with profilometers that are capable of recording raw surface profiles without removing longer spatial wavelengths. For instance, the widely used skidded stylus profilometers are not suitable for this task.[17] Two different types of surface profilers that fulfil this boundary condition were used in this study. In all measurements, the surface profiles were recorded orthogonal to the direction of the tensile elongation.

A vertical scanning white light interferometer Veeco WYKO NT1100 was the mainly-used profilometer in this study. This optical 3D-profilometer was equipped with a motorized sample stage having maximum displacements of 102 mm in the x and y directions. A Michelson type interferometer objective with 5x magnification and a 0.5x field-of-view lens resulting in a 2.5x overall magnification was used to record a track of 41 3D-profiles with a size of 2.45 × 1.86 mm, each. The data point spacing was 3.32 × 3.87 μm corresponding to 736 × 480 data points in every 3D-profile. The 41 profiles were stitched together using the Veeco Vision 3.60 software resulting in a total profile length of 80.02 mm and a width of 1.86 mm. Examples are shown in Fig. 1 below the sample photographs. The exported 2D-profiles were the average of all 480 parallel 80.02 mm long lines in the original 3D-profile resulting in a 2D-profile width of 1.86 mm. This measure reduced the influence of small surface defects in the 3D-profile on the final 2D-profile, which consisted of 24103 measurement points at an interval of 3.32 μm.

A non-skidded bench-top 2D stylus profilometer Zeiss Surfcom 2000 SD3 served as the second instrument. It is capable of recording directly unfiltered 2D raw profiles with a length of 80.07 mm at a transverse speed of 1.0 mm/s. The stylus tip had a radius of 2 μm. The measured profiles consisted of 31775 data points with a spacing of 2.52 μm.

2.3. Evaluation of the Surface Profiles

The 2D raw profiles of strained ridging test specimens contain three components: the overall shape of the specimen, the ridging profile itself and the residual profile which is caused by the surface roughness of the sample and instrument noise. Cubic spline fitting and interpolation, which is considered to be a suitable method for surface profile filtering, was applied to separate the ridging profile from the shape of the specimen and from surface roughness and instrument noise. Compared to Gaussian filters, which are widely applied in surface roughness measurements, spline filtering has the advantage that artifacts are rarely introduced. Consequently, the whole traversing length can be evaluated without the need for run-in and run-out periods. For the shape removal,[18,19] the distance between the breakpoints of the cubic spline fit was set to 3.3 mm assuring that the commonly smaller ridging surface features were not disturbed unreasonably by the fitting procedure. The difference between this first spline fit and the raw profile gives an intermediate profile, which has already a proper center line. It contains, however, not only the desired ridging information but also the roughness and noise components of the measurement. The final ridging profile is extracted from the intermediate profile by a second spline fit. The difference between the breakpoints for removing the surface roughness and instrument noise parts was set to 0.33 mm. Finally, a clean profile that contains only the main surface features caused by the ridging phenomenon is received for further processing.

The filtered ridging profile is the base for calculating the ridging index *RI* as a measure of the intensity of the surface defect. As ridging is more detrimental when the valleys between the ridges are deeper, the profile height surface parameter *Rz* is calculated. A procedure similar to that in ISO 4287:1997[20] was adapted with the goal of limiting the influence of local extreme values on the result. The ridging profile is divided into five equal parts with a length of 16 mm, each. The deepest valley and the highest peak of each section is determined. The sum of the absolute value of the average valley depth *Rv* and the average peak height *Rp* over the five sections gives *Rz*. As more ridges and valleys make the ridging surface defect more difficult to remove, the peak count *Pc* is computed from the ridging profile. The roughness average *Ra* of the residual roughness and noise profile, multiplied by 2, is used as threshold to determine *Pc*. The dimensionless *RI* is then defined as the product of *Rz* in μm and *Pc* in mm^{-1}:

$$RI = Rz\,[\mu m] \times Pc\,[mm^{-1}]$$

Spline fitting and interpolation as well as the computation of *Rz*, *Pc* and *RI* was achieved with a Scilab 6[21] script using the built-in functions *lsq_splin* and *interp* for spline filtering. A short example script is available from the authors on request.

3. Results and Discussions

3.1. Evaluation

A detailed example for the used surface profile filtering procedure by spline interpolation is shown in **Fig. 2**. The grade EN 1.4016 FSS sample is the same as presented in Fig. 1(b) after 15% elongation. The raw profile had been measured using the optical 3D profilometer. The first cubic spline fit for the removal of the shape from the recorded raw profile is illustrated in Figs. 2(a) to 2(c). The ridging profile is produced by the second spline fit which eliminates the surface roughness and noise components (see Figs. 2(d) to 2(f)). The resulting curve (see Fig. 2(e)) is used to derive *Rz* and *Pc* for the calculation of *RI*. The threshold for the calculation of *Pc* is indicated in Fig. 2(e). An *RI* value of 7.6 was determined based on an *Rz* value of 20.1 μm and a *Pc* of 0.38 mm^{-1}.

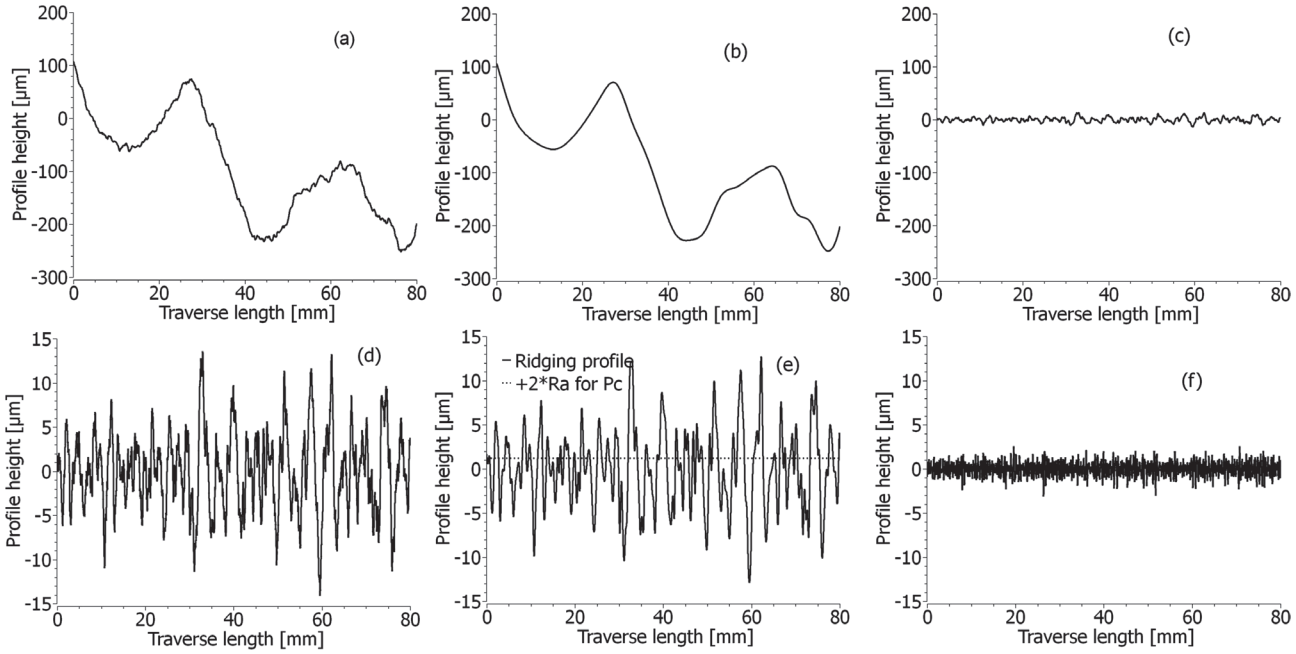

Fig. 2. Illustration of the filtering procedure based on spline interpolation and fitting using a 2D profile extracted from a measurement with the optical 3D profilometer. The upper row shows the removal of the form of the sample: (a) recorded raw profile, (b) spline fit to remove the form, (c) intermediate ridging profile containing surface roughness and instrument noise. The subtraction of the surface roughness and instrument noise from the intermediate ridging profile is shown in the lower row: (d) intermediate ridging profile (same curve as in plot (c)), (e) filtered ridging profile and (f) residual surface roughness and instrument noise. The filtered ridging profile (e) is used to compute *Rz*, *Pc* and *RI*. The threshold for the calculation of Pc is indicated in (e) by the horizontal line.

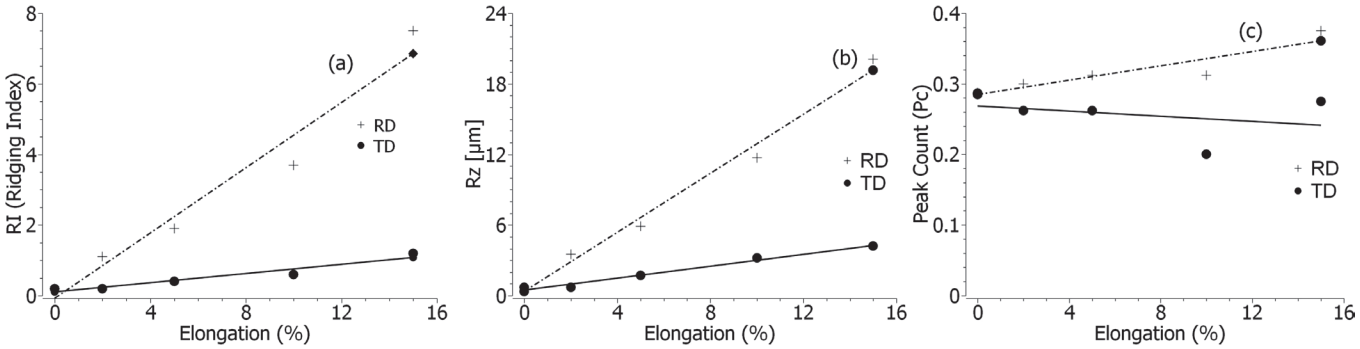

Fig. 3. Dependence of (a) *RI*, (b) *Rz* and (c) *Pc* on the elongation of the sample.

3.2. Influence of Strain and Straining Direction

As the intensity of ridging is expected to be a function of the elongation of the sample, a series of measurements with the same FSS sheet after elongations of 0%, 2%, 5%, 10% and 15% was recorded with the optical 3D profilometer. Additionally, a second set of specimens was strained parallel to TD instead of RD as a blind test with samples that did not show the ridging problem. They had been strained to the same elongations as before leading only to random surface roughening[22,23] which normally occurs during forming operations. As **Figs. 3**(a) and 3(b) show, *RI* and *Rz* depend linearly on the applied elongation. *Pc* is nearly constant and grows only slightly (see Fig. 3(c)) indicating that the number of ridges is constant during the tensile test. As expected, the highest *RI* was determined for the highest elongation in the test series. To maximize the sensitivity and resolution of the test method, all ridging measurements were done thereafter with an elongation of 15%. As an *RI* of around 1 can even be found on ridging-free samples strained to 15%, specimens with $RI \leq 1$ are considered to be ridging-free.

3.3. Dependence on Sheet Side Tested

The ridging profiles of both surfaces of another sample were measured with the optical 3D profilometer to identify the influence of the examined side of the specimen on the measurements. The determined *RI* as well as the surface parameters *Rz* and *Pc* are listed in **Table 1**. The similarity of the results indicates that the determined values do not depend on the measured surface of the specimen. As the filtered ridging profiles plotted in **Fig. 4** show, the peaks on one side of the sample correspond to valleys on the other side and vice versa.

3.4. Validation

To study the repeatability of the proposed profilometric ridging test method, a grade EN 1.4016 FSS sheet was measured at different positions as indicated in **Fig. 5**(a). The specimen which was cut from the center of a 1250 mm

wide sheet was studied after 15% elongation six times with a spacing between the profile lines of 10 mm in RD. An average *RI* of 4.4 was determined (see Fig. 5(b)). The results of the six single measurements varied between 4.2 and 4.7 and the results are tabulated in **Table 2**. The *RI*'s of all seven specimens that were cut across the sheet width are shown in Fig. 5(c) and the results are also tabulated in **Table 3**. Four of the six additional specimens had similar *RI*'s to the center sample. The two samples that had been cut 250 mm and 350 mm from the center of the sheet width showed about one-unit higher *RI* values. As the other measurements all produced very similar results, this variation has to be

Table 1. *Rz*, *Pc* and *RI* values determined for the upper and lower sides of the same strained specimen.

	Rz [μm]	Pc [mm^{-1}]	RI
Upper side	13.8	0.38	5.2
Lower side	15.4	0.33	5.0

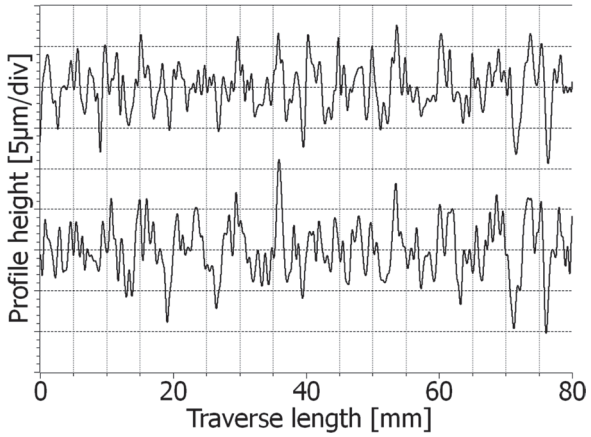

Fig. 4. Filtered ridging profiles of the upper and lower sides of the same strained sample. The curve of the lower side has been inverted to illustrate better the correlation between the ridges and valleys on the two sides of the specimen.

Table 2. Results of the evaluated ridging index (RI) from surface profile measurements conducted with an interval of 10 mm along the rolling direction (RD) on the same specimen.

No. of measurement	Ra (μm)	Rz (μm)	Pc	RI
1	0.30	15.7	0.30	4.7
2	0.29	16.1	0.29	4.6
3	0.33	15.4	0.29	4.4
4	0.29	16.0	0.28	4.4
5	0.29	13.9	0.30	4.1
6	0.31	14.1	0.30	4.2
Average	0.30	15.2	0.29	4.4

Table 3. The variation of measured surface parameters and the evaluated RI across the width of sheet of the specimens as shown in Fig. 5(a).

Location of measurement	Ra (μm)	Rz (μm)	Pc	RI
C+5	0.27	13.5	0.31	4.2
C+4	0.29	17.2	0.31	5.4
C+3	0.31	17.3	0.31	5.4
C+2	0.30	19.8	0.21	4.2
C+1	0.33	17.3	0.26	4.5
C0−Avg	0.30	15.2	0.29	4.4
C−1	0.30	15.0	0.30	4.5

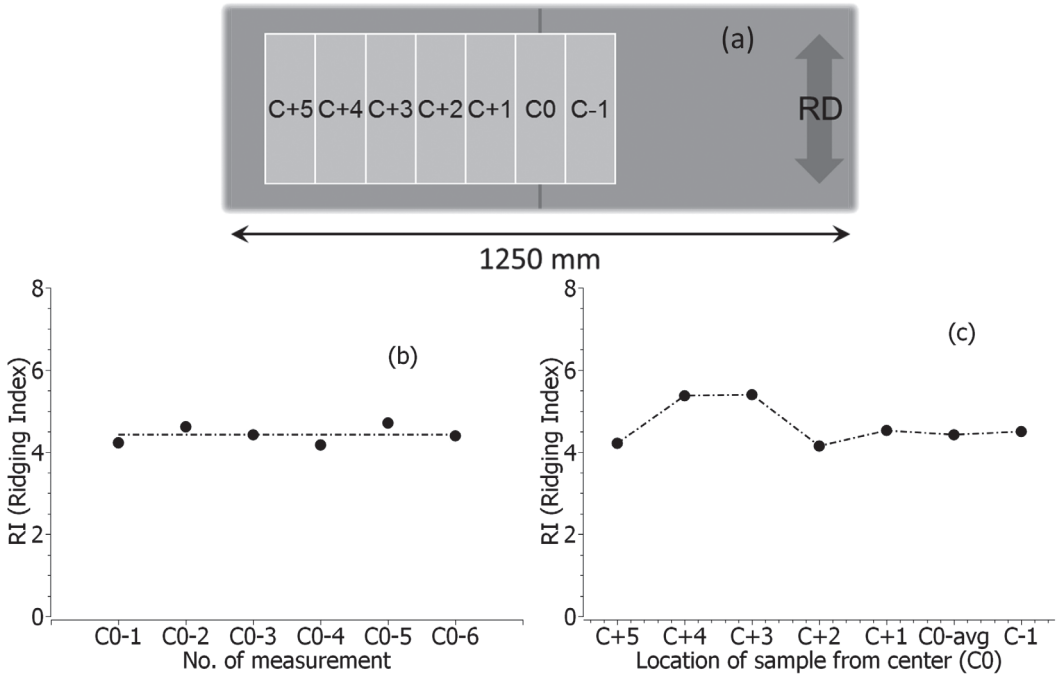

Fig. 5. Ridging measurements on seven samples which were cut from a 1250 mm wide grade EN 1.4016 FSS sheet. (a) Positions of the samples in the 1250 mm wide FSS sheet, (b) result of six parallel ridging measurements and their average value (dashed line) of sample C0, (c) variation of *RI* across the seven samples.

considered as significant indicating perhaps a locally different texture in the studied FSS sheet.

To verify the influence of the type of profilometer on the proposed measurement procedure, 36 FSS sheets which had been strained to 15% along the RD resulting in different degrees of ridging were measured with the 2D stylus profilometer and the optical 3D profilometer. The determined *RI*'s are plotted in **Fig. 6**(a). The measured *RI* values of these specimens varied mostly between 0 and 8. *RI*'s higher than 10 were rarely encountered. The correlation coefficient R^2 between the evaluated *RI*'s using both the measuring instruments is 0.97. The observed deviations between both the measurement techniques is always below 1.5 *RI* units and below about 10% of the measured *RI* value.

As R^2 only measures the strength of a relation between two variables but not the agreement between them, a Bland-Altman plot[24] of the ridging indices evaluated with the proposed method using two different measurement techniques was prepared as shown in Fig. 6(b). The mean difference *d* and standard deviation *s* were −0.26 and 0.52, respectively, for *RI* evaluated using the two measurement techniques. The limits of agreement between the two measurements is such that the *RI* deviated from the 2D profilometer could be either 0.77 units higher or −1.29 units lower than data generated by the 3D profilometer. As these deviations are very small, it can be stated that the proposed surface profile evaluation method for calculating *RI* is sufficiently independent of the technique that is used to record the surface profile.

The ridging defect can be seen on the surface of the sidewalls of deep drawn products. During deep drawing, the direction of the strain is constantly changing with respect to the rolling direction of the sheet. For example, the strain direction is the same as the rolling direction of the sheet where ridging is at its maximum. There are two such positions opposite each other in a circular deep drawn pot. The present method cannot be used to measure the ridging index of the deep drawn product, due to the limitation of the measurement equipment and due to the curvature of the product. The sample could be straightened after cutting for the measurement, even then it is not representative due to constant change in strain direction in the sample. The polishing demand for the deep drawn product cannot be predicted by the ridging measurement of the specimen due to the flattening of the profile during the deep drawing process. However, the presented ridging test method can be used for process optimization and quality control in the production and as tool for material acceptance to assure that suitable raw material can be chosen, thus reducing polishing cost. Practical experience shows that the material with ridging index less than 1 does not require any additional polishing other than to remove the roughening caused by deep drawing.

3.5. Comparison with Visual Assessment Results

A set of five samples from different batches with different degrees of ridging was selected for a comparison between the proposed profilometric ridging measurement method and the commonly applied visual inspection and rating of strained FSS samples. 100 mm wide specimens were elongated to 15% and rated by five test persons who were familiar with the visual inspection of stainless steel surfaces.

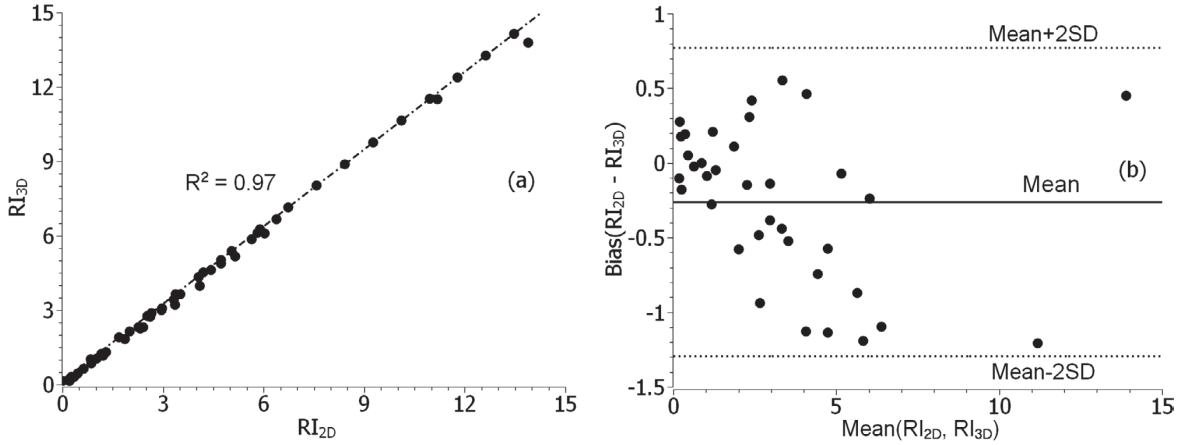

Fig. 6. Ridging indices of 36 FSS sheet samples measured with the 2D stylus profilometer (RI_{2D}) and the optical 3D profilometer (RI_{3D}). (a) Plotted against each other demonstrating a good correlation. (b) Bland-Altman plot between the average and the difference between RI_{2D} and RI_{3D} to find the limits of agreement between the surface profile measurement techniques.

Table 4. Results of the visual inspection and rating of five sheets from different batches strained to 15% along RD, (scale between 0 and 10) with different intensity of the surface defect. The measured RI is given for comparison.

Sample	Person 1	Person 2	Person 3	Person 4	Person 5	Average	Ra (μm)	Rz (μm)	Pc	RI
A	4	3	3	2	2	2.8	0.46	9.6	0.22	2.1
B	9	7	5	9	5	7.0	0.35	25.5	0.30	7.5
C	1	0	1	1	1	0.8	0.11	4.2	0.28	1.2
D	8	5	3	7	4	5.4	0.48	13.7	0.27	3.7
E	7	5	8	3	8	6.2	0.35	11.1	0.40	4.4

The test persons were instructed to use an arbitrary scale between 0 and 10. The samples could be examined simultaneously, but reference specimens were not provided. The results are listed together with the determined *RI*'s in **Table 4**. The variation between the ratings of different persons was in some cases huge. However, the average result produced by the reference group and *RI*'s determined by the optical 3D profilometer gave the same ranking between the specimens. The average rating numbers correlated well with the *RI*'s. The biggest deviations were observed with specimens D and E, which exhibited medium ridging intensities.

4. Conclusions

The ridging surface defect which may form on FSS after elongation in RD to 15% can be measured using a surface profilometer in a reliable and reproducible way by using 100 mm wide samples. The ridging profile is derived from the recorded raw profile using two spline filtering steps, which remove the form of the specimen as well as the surface roughness and instrument noise components. A ridging index *RI* is calculated by taking into account the height of the filtered profile and the spacing between the ridges.

The defined *RI* is a linear function of the elongation of the specimens in RD. The introduced method does not depend on which side of the sheet specimen is studied or on the profilometer type used as long as the profilometer allows an unfiltered surface profile to be recorded. The reproducibility of the measurement results is sufficiently good. The determined values correspond well with results from visual ridging assessments without showing the scatter typically observed when different persons perform the visual rating.

REFERENCES

1) H. J. Shin, S. H. Hong and D. N. Lee: *Key Eng. Mater.*, **274**–**276** (2004), 11.
2) G. Lefebvre, C. W. Sinclair, R. A. Lebensohn and J-D. Mithieux: *Model. Simul. Mater. Sci. Eng.*, **20** (2012), 024008.
3) H. Chao: *Trans. Am. Soc. Met.*, **60** (1967), 37.
4) H. J. Shin, J. K. An, S. H. Park and D. N. Lee: *Acta Mater.*, **51** (2003), 4693.
5) M. Brochu, T. Yokota and S. Satoh: *ISIJ Int.*, **37** (1997), 872.
6) S. H. Park, K. Y. Kim, Y. D. Lee and C. G. Park: *ISIJ Int.*, **42** (2002), 100.
7) J. Hamada, Y. Matsumoto, F. Fudanoki and S. Maeda: *ISIJ Int.*, **43** (2003), 1989.
8) T. Tsuchiyama, R. Hirota, K. Fukunaga and S. Takaki: *ISIJ Int.*, **45** (2005), 923.
9) J. Mola, I. Jung, J. Park, D. Chae and B. C. de Cooman: *Metall. Mater. Trans. A*, **43** (2012), 228.
10) S. Patra and L. K. Singhal: *Mater. Sci. Appl.*, **4** (2013), 70.
11) Y. Itoh, T. Okajima, H. Maede and K. Tashiro: *Trans. Iron Steel Inst. Jpn.*, **22** (1982), 223.
12) P. D. Wu, D. J. Lloyd, A. Bosland, H. Jin and S. R. MacEwen: *Acta Mater.*, **51** (2003), 1945.
13) Y. Shi, H. Jin, P. D. Wu and D. J. Lloyd: *Acta Mater.*, **124** (2017), 598.
14) G. J. Baczynski, R. Guzzo, M. D. Ball and D. J. Lloyd: *Acta Mater.*, **48** (2000), 3361.
15) Y. S. Choi, H. R. Piehler and A. D. Rollett: *Mater. Charact.*, **58** (2007), 901.
16) A. Guillotin, G. Guiglionda, C. Maurice and J. H. Driver: *Mater. Charact.*, **61** (2010), 1119.
17) The American Society of Mechanical Engineers: Surface Texture (Surface Roughness, Waviness, and Lay), ASME B46.1-2009, ASME, New York, NY, (2010), 25.
18) D. J. Whitehouse: Handbook of Surface Metrology, IOP Publishing, Bristol, (1994), 27.
19) M. Krystek: *Measurement*, **18** (1996), 9.
20) ISO 4287:1997, Gemoetrical Product Specifications (GPS) – Surface texture: Profile method – Terms, definitions and surface texture parameters.
21) C. C. Bordeianu, C. Beşliu, A. Jipa, D. Felea and I. V. Grossu: *Comput. Phys. Commun.*, **178** (2008), 788.
22) N. Kawai, T. Nakamura and Y. Ukai: *Bull. JSME*, **29** (1986), 1337.
23) R. Mahmudi and M. Mehdizadeh: *J. Mater. Process. Technol.*, **80**–**81** (1998), 707.
24) J. Martin Bland and D. Altman: *Lancet*, **327** (1986), 307.